ARTICLE

Electron Momentum Spectroscopy of Outer Valence Orbitals of 2-Fluoroethanol

Yu-feng Shi[a], Xu Shan[a,b]*, En-liang Wang[a,b], Hong-jiang Yang[a], Wei Zhang[a], Xiang-jun Chen[a,b]

a. Hefei National Laboratory for Physical Sciences at the Microscale and Department of Modern Physics, University of Science and Technology of China, Hefei 230026, China
b. Synergetic Innovation Center of Quantum Information and Quantum Physics, University of Science and Technology of China, Hefei 230026, China

(Dated: Received on October 10, 2014; Accepted on November 4, 2014)

The binding energy spectra and electron momentum distributions for the outer valence molecular orbitals of gaseous 2-fluoroethanol have been measured by the non-coplanar asymmetric (e, 2e) spectrometer at impact energy of 2.5 keV plus binding energy. The quantitative calculations of the ionization energies and the relevant molecular orbitals have been carried out by using the outer-valence Green's function method and the density functional theory with B3LYP hybrid functional. The observed ionization bands in binding energy spectra, as well as the previous photoelectron spectrum which was not assigned, have been assigned for the first time through the comparison between experiment and theory. In general, the theoretical electron momentum distributions calculated by B3LYP method with aug-cc-pVTZ basis set are in line with the experimental ones when taking into account the Boltzmann-weighted thermo-statistical abundances of five conformers of 2-fluoroethanol.

Key words: (e, 2e) Electron momentum spectroscopy, 2-Fluoroethanol, Conformer, Density functional theory

I. INTRODUCTION

Electron momentum spectroscopy (EMS), also known as binary (e, 2e) spectroscopy, is a powerful technique for exploring the electronic structures of atoms and molecules [1–4]. The principal value of the EMS for understanding the electron behavior lies in its unique ability to obtain directly both the binding energy spectra and the electron density distributions in momentum space for individual orbitals [1–4]. Such information is useful for the assignment of the ionic states of atoms and molecules, evaluation of the quality of different types of quantum chemical calculations, as well as the understanding of phenomena such as chemical reactivity and molecular recognition. In the past decades, EMS has been extensively used to study the conformational effect on the electronic structure of molecules such as *n*-glycine [5, 6], *n*-butane [7, 8], 1-butene [9–11], tetrahydrofurane [12–14], ethylamine [15], ethanethiol [16], and ethanol [17–20]. When taking into account the Boltzmann-weighted population for different conformers, the thermally averaged theoretical momentum distributions are usually in accordance with the experimental results. However, in the case of ethanol, the calculations failed to reproduce the experiment quantitatively [18, 19]. Recently, molecular dynamical simulations of Hajgato *et al.* [20] improved the agreement of theory with experiment in view of the ultrafast nuclear dynamics. But the discrepancy between theory and experiment still remained. It therefore needs more EMS experimental information on structural versatile molecules for further theoretical studies on such phenomena.

2-Fluoroethanol (2-FE), a derivative of ethanol in which one hydrogen of methyl group is replaced by a fluorine atom, has five conformers existing in this molecule as shown in Fig.1. The conformational arrangement of C−F bond rotation about the C−C bond is denoted as G (Gauche) or T (Trans). The arrangement of O−H bond rotation about the C−O bond is denoted as either g (*gauche*) or t (*trans*). In the case of a G arrangement about the C−C bond, there are two inequivalent conformers with respect to the C−O bond and differentiated as g or g′. Many theoretical and experimental works were devoted to the molecular geometries and conformational energies of 2-FE [21–28] and it was concluded that the Gg′ conformer is the most stable one with about 90% population. However, studies of the electronic structure of 2-FE are very scarce. There is only one report on the photoelectron spectrum (PES) measured by He I ultraviolet radiation [29], but the observed ionization bands were not assigned. It is worth noting that EMS can provide an effective way to assign the bands ionized from molecular orbitals by simply

*Author to whom correspondence should be addressed. E-mail: xshan@ustc.edu.cn

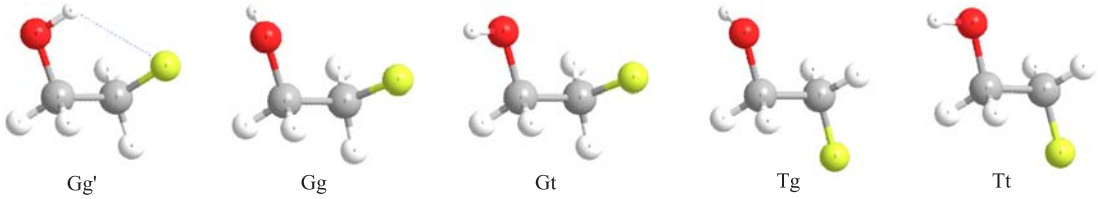

FIG. 1 Geometry structures of five conformers including Gg′, Gg, Gt, Tg, and Tt of 2-FE optimized by MP2/aug-cc-pVTZ.

comparing the experimental electron momentum distributions with the theoretical ones [30–33]. Therefore, it is necessary to carry out the detailed EMS studies on electronic structures of 2-FE molecule both experimentally and theoretically.

In the present work, we report the first EMS measurement on binding energy spectra and electron momentum distributions for the outer valence molecular orbitals of gaseous 2-FE. The experimental results are interpreted on the basis of the quantitative calculations of the ionization energies and the relevant molecular orbitals using the outer-valence Green's function method [34–36] and the density functional theory with B3LYP hybrid functional [37–40].

II. EXPERIMENTAL AND THEORETICAL BACKGROUND

EMS is based on the high-energy electron impact single ionization process, in which the kinematics of all the electrons is fully determined. The present experiment on 2-FE molecule is carried out by using the noncoplanar asymmetric (e, 2e) spectrometer which was described in detail elsewhere [33, 41] and thus only a brief description is given here. The incident electron beam generated from an electron gun is accelerated by an electrostatic lens system to the desired energy of 2.5 keV plus binding energy, and transferred to the reaction region where it impacts with the gas-phase target molecules injected by a nozzle. The scattered electron outgoing along polar angle $\theta_{\rm a}$=14° passes through the fast electron analyzer and is detected by a two dimensional position sensitive detector (PSD) over a large range of both energies and azimuthal angles of interest. The ionized electron outgoing along polar angle $\theta_{\rm b}$=76° passes through the slow electron analyzer and is detected by one dimensional PSD. In such experimental condition, considering conservation of energy and momentum, the binding energy ε and magnitude of momentum p of target electron can be expressed by

$$\varepsilon = E_0 - E_{\rm a} - E_{\rm b} \tag{1}$$

$$p = [p_0^2 + {p_{\rm a}}^2 + {p_{\rm b}}^2 - 2p_0p_{\rm a}\cos\theta_{\rm a} - 2p_0p_{\rm b}\cos\theta_{\rm b} + 2p_{\rm a}p_{\rm b}(\cos\theta_{\rm a}\cos\theta_{\rm b} - \sin\theta_{\rm a}\sin\theta_{\rm b}\cos\phi)]^{1/2} \tag{2}$$

where (E_0, p_0), ($E_{\rm a}$, $p_{\rm a}$), and ($E_{\rm b}$, $p_{\rm b}$) are the energies and momenta of the projectile, scattered, and ejected electrons, respectively. And ϕ is the relative azimuthal angle between the two outgoing electrons. Therefore, by detecting two outgoing electrons in coincidence, the binding energy and momentum of the target electron can be determined. Before the experiment of 2-FE, the energy and momentum resolutions of the present EMS spectrometer are determined to be ∼1.0 eV (full width at half maximum (FWHM)) and ∼0.1 a.u., respectively, by measuring the ionization spectra and electron momentum distributions of Ar3p orbital.

On the theoretical side, with the binary encounter approximation and the plane wave impulse approximation (PWIA), as well as the target Hartree-Fock or Kohn-Sham approximation, the triple differential cross-section (TDCS) of (e, 2e) process can be described as Ref.[1–4]:

$$\sigma_{\rm EMS} \propto S_j^{(f)} \int |\psi_j(\mathbf{p})|^2 \, {\rm d}\Omega \tag{3}$$

where $\psi_j(\mathbf{p})$ is the one-electron canonical Hartree-Fock or Kohn-Sham wave function in momentum space for the jth orbital from which the electron is knocked out. $S_j^{(f)}$, known as spectroscopic factor or pole strength, denotes the possibility of forming a one-hole configuration in the final state f. The integral in Eq.(3) is usually referred to as the spherically averaged one-electron momentum distribution, *i.e.*, electron momentum profile.

For 2-FE molecule, in the previous studies, the theoretical calculations [21–24] predicted that it had Gg′, Gg, Tg, Gt, and Tt five conformers. Whereas experiments [24–28] determined the most stable Gg′ conformer to be ∼90% abundance, and the Tt or Tg conformer was less than 10%. In the present calculations, the structural parameters and energies of these conformers are optimized at benchmark theoretical level using the second-order Møller-Plesset perturbation (MP2) [42] method with large basis set of aug-cc-pVTZ [43]. The optimized structural parameters agree well with the available data from electron diffraction [25, 26] and microwave spectra [27]. The calculated energies of five conformers, in which the zero-point vibrational energy correction and the thermodynamics enthalpy correction are taken into account, are used to estimate the relative abundance n_i with the Boltzmann statistics according to the equation

$$n_i = \rho_i \exp\left(\frac{\Delta E}{k_{\rm B}T}\right) \tag{4}$$

DOI:10.1063/1674-0068/28/cjcp1410175

where k_B is the Boltzmann constant, T is temperature, ρ_i is the symmetry number of conformers, and ΔE is the energy difference relative to the most stable conformer Gg′. At room temperature, the relative abundances of conformers are deduced to be 91.1% Gg′, 1.8% Gg, 4.1% Tg, 1.7% Gt and 1.2% Tt, respectively. Furthermore, based on the optimized molecular geometries of the respective conformers, the position space Kohn-Sham wave functions are calculated by using DFT-B3LYP method with aug-cc-pVTZ basis set. Thus, the theoretical momentum profiles for the outer valence molecular orbitals (MOs) of five conformers of 2-FE are obtained according to Eq.(3). All the theoretical calculations are carried out using the Gaussian 03 suite of programs [44].

III. RESULTS AND DISCUSSION

A. Binding energy spectra

2-FE (CH_2FCH_2OH) contains 34 electrons and has nine outer valence molecular orbitals (MOs). B3LYP calculations indicate that the ground state electronic configurations of Gg′, Gg, Tg and Gt conformers having C_1 symmetry point group can be written as

$$(\text{core})^8 \underbrace{(5a)^2\,(6a)^2\,(7a)^2\,(8a)^2}_{\text{Inner-valence}} \underbrace{(9a)^2\,(10a)^2\,(11a)^2\,(12a)^2\,(13a)^2\,(14a)^2\,(15a)^2\,(16a)^2\,(17a)^2}_{\text{Outer-valence}} \tag{5}$$

and Tt conformer having C_s symmetry point group can be written as

$$(\text{core})^8 \underbrace{(5a')^2(6a')^2(7a')^2(8a')^2}_{\text{Inner-valence}} \underbrace{(9a')^2(1a'')^2(10a')^2(11a')^2(2a'')^2(12a')^2\,(3a'')^2(13a')^2(4a'')^2}_{\text{Outer-valence}} \tag{6}$$

The binding energy spectra (BES) for the outer valence MOs of 2-FE in the energy range of 9−20 eV have been measured simultaneously in the desired range of azimuthal angles, and the summed over all the azimuthal angles ϕ is shown in Fig.2(b), together with the previous PES spectrum [29] in Fig.2(a) and the simulated spectra in Fig.2(c). The vertical ionization potentials (IPs) for the outer valence MOs of Gg′, Gg, Tg, Gt, and Tt five conformers have been calculated using OVGF method with 6-311++G** basis set. As listed in Table I, the calculated IPs are very close to each other for the relevant MOs of the five conformers which could contribute to the same ionization bands in BES. Due to the energy resolution of 1.0 eV (FWHM) of present EMS spectrometer, four obvious lobes in Fig.2(b) are observed in BES, which contain the contributions from

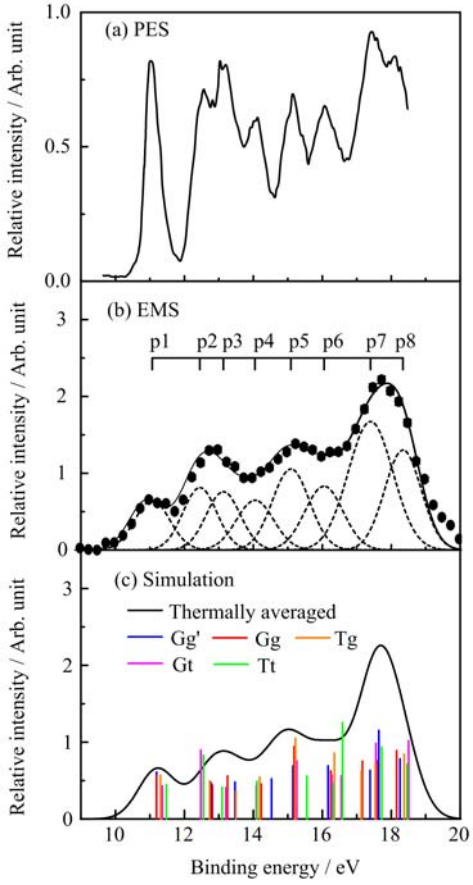

FIG. 2 Binding energy spectra for the outer valence orbitals of 2-FE. (a) The previous PES spectrum [29]. (b) The present BES measured over all ϕ angles by EMS. The dashed lines represent Gaussian peaks fitting the BES and the solid line is the summed fit. The vertical bars indicate the positions of Gaussian peaks. (c) The theoretical simulated BES based on OVGF/6-311++G** calculation, in which the relative abundance of Gg′, Gg, Gt, Tg and Tt was taken into account. The positions of vertical bars denote the calculated ionization energies for the individual conformer and the height represents the product of the pole strength and the density of states.

nine overlapping ionization bands in the outer valence region. Although more ionization bands were resolved by the previous PES in Fig.2(a), they were not assigned [29]. It is preferable to resort to the theoretical simulations at the OVGF/6-311++G** level for analyzing and assigning the observed structures in the available EMS and PES spectra. Figure 2(c) shows the simulated BES constructed by convoluting the calculated results, using Gaussian function as the convolution function with the width of 1.0 eV (FWHM) from the EMS instrumental resolution. The positions of Gaussian functions, as the vertical bars in Fig.2(c), are from the IPs of the five conformers as listed in Table I, and the intensities are from the product of pole strengths and densities of states. The solid curve is the thermally averaged theo-

DOI:10.1063/1674-0068/28/cjcp1410175

TABLE I Experimental and theoretical IPs for outer valence MOs of 2-FE molecule.

Experimental IP			Theoretical (OVGF/6-311++G**)[a] IP						
Peak	EMS[a]	PES[b]	MO	C_1/C_s	Gg′ (C_1)	Gg (C_1)	Tg (C_1)	Gt (C_1)	Tt (C_s)
p1	11.1	11.1	17	17a/4a″	11.20[0.92]	11.20[0.92]	11.31[0.92]	11.36[0.93]	11.48[0.93]
p2	12.5	12.5	16	16a/13a′	12.77[0.92]	12.82[0.92]	12.73[0.93]	12.48[0.92]	12.55[0.92]
p3	13.2	13.2	15	15a/3a″	13.47[0.93]	13.25[0.93]	13.50[0.92]	13.20[0.93]	13.10[0.93]
p4	14.1	14.1	14	14a/12a′	14.53[0.92]	14.23[0.92]	14.18[0.92]	14.09[0.92]	14.11[0.92]
p5	15.1	15.1	13	13a/2a″	15.15[0.92]	15.18[0.92]	15.22[0.92]	15.26[0.92]	15.56[0.92]
p6	16.1	16.1	12	12a/11a′	16.17[0.92]	16.25[0.92]	16.35[0.92]	16.27[0.92]	16.32[0.92]
p7	17.4	17.4	11	11a/10a′	17.39[0.92]	17.16[0.92]	17.13[0.92]	16.55[0.92]	16.58[0.92]
			10	10a/1a″	17.64[0.92]	17.58[0.92]	17.54[0.92]	17.55[0.92]	17.73[0.92]
p8	18.3	18.2	9	9a/9a′	18.25[0.92]	18.16[0.92]	18.38[0.92]	18.50[0.92]	18.46[0.92]

[a] This work. Pole strengths are listed in square brackets.
[b] The IPs values are obtained by fitting the PES spectrum [29] with eight Gaussian functions.

retical spectra including the contribution of 91.1% Gg′, 1.8% Gg, 4.1% Tg, 1.7% Gt and 1.2% Tt conformers. In general, the simulated ionization spectra can reproduce the experimental BES well.

In order to extract the experimental electron momentum profiles for the outer valence MOs of 2-FE, Gaussian functions are used to fit the BES as shown by the dashed curves in Fig.2(b) and the overall fitted spectrum is represented by the solid line. The positions of Gaussian peaks (p1−p8) are referred to the IPs obtained by fitting the high-resolution PES [29], and the widths are the combination of EMS instrumental energy resolution and Franck-Condon widths of the ionization bands deduced from PES spectra. Slight adjustments have been applied to compensate the asymmetries of the shapes of the Franck-Condon profiles. As shown in Fig.2(b), the first band (p1) at 11.1 eV is well resolved and corresponds to the ionization of the highest occupied molecular orbital (HOMO). In the region of 12−17 eV, there are two lobes which contain five unresolved peaks (p2−p6) corresponding to MO16−MO12 due to the limited energy resolution of EMS spectrometer. For the last lobe two Gaussian functions are fitted, which contains three outer valence orbitals, *i.e.* MO11−MO9. According to the OVGF calculation, the ionization band (p7) at 17.4 eV should be ascribed to the cooperative contributions from MO11 (11a/10a′) and MO10 (10a/1a″), and the one (p8) at 18.3 eV should be ascribed to MO9 (9a/9a′). Further assignments of the observed bands will be presented in next section by comparing the experimental and theoretical momentum profiles. The determined ionization energies and band assignments are also presented in Table I.

B. Experimental and theoretical electron momentum profiles

The experimental momentum profiles (XMPs) for each peak (p1−p8) are extracted by deconvoluting a series of angular correlated BES, and plotting area under the corresponding fitted peak as a function of momentum p (*i.e.*, ϕ angle). The theoretical momentum profiles (TMPs) for the outer valence MOs of the five conformers are calculated using the B3LYP method with the basis set of aug-cc-pVTZ. For the sake of comparison, the TMPs are folded with the instrumental momentum resolution using the Gaussian weighted planar grid method [45, 46]. In addition, the XMPs and the TMPs are placed on a common intensity scale using an uniform factor obtained by normalizing the summed XMPs for p1−p8 to the summed TMPs for MO17−MO9, in which the relative abundances of 91.1% Gg′, 1.8% Gg, 4.1% Tg, 1.7% Gt, and 1.2% Tt deduced by MP2/aug-cc-pVTZ calculations are also taken into account. The XMPs and the corresponding TMPs for the outer valence MOs of 2-FE are shown in Fig.3. It is noted that the error bars of experimental data given in the figures represent the overall error of the statistical and deconvolution uncertainties. In addition, the molecular orbital maps in position space for each of conformers calculated by B3LYP/aug-cc-pVTZ are illustrated in Fig.4.

Figure 3(a) presents the XMP for the first ionization band (p1) together with the corresponding TMPs for HOMO (*i.e.*, MO17), of which the lone pair of oxygen 2p predominates. The individual TMPs of five conformers appear two remarkably different characteristics. For *trans* geometrical arrangements (t) due to the O−H rotation about C−O bond, *i.e.*, Gt and Tt, TMPs show 'p-type' character, similar to the profile of oxygen 2p lone pair. While for *gauche* arrangements (g or g′), *i.e.*, Gg′, Gg, and Tg, TMPs exhibit 'sp-type' profiles. The thermally averaged TMP shows an 'sp-type' character, and can reproduce the XMPs well except at p<0.25 a.u. It is worth noting that the XMP feature for HOMO of 2-FE molecule is almost the same as the case of ethanol [17]. The O−H internal rotation about C−O bond leads to the obvious change of electron density distributions for *gauche* and *trans* conformers. This should also be ascribed to the hyperconjugative inter-

DOI:10.1063/1674-0068/28/cjcp1410175

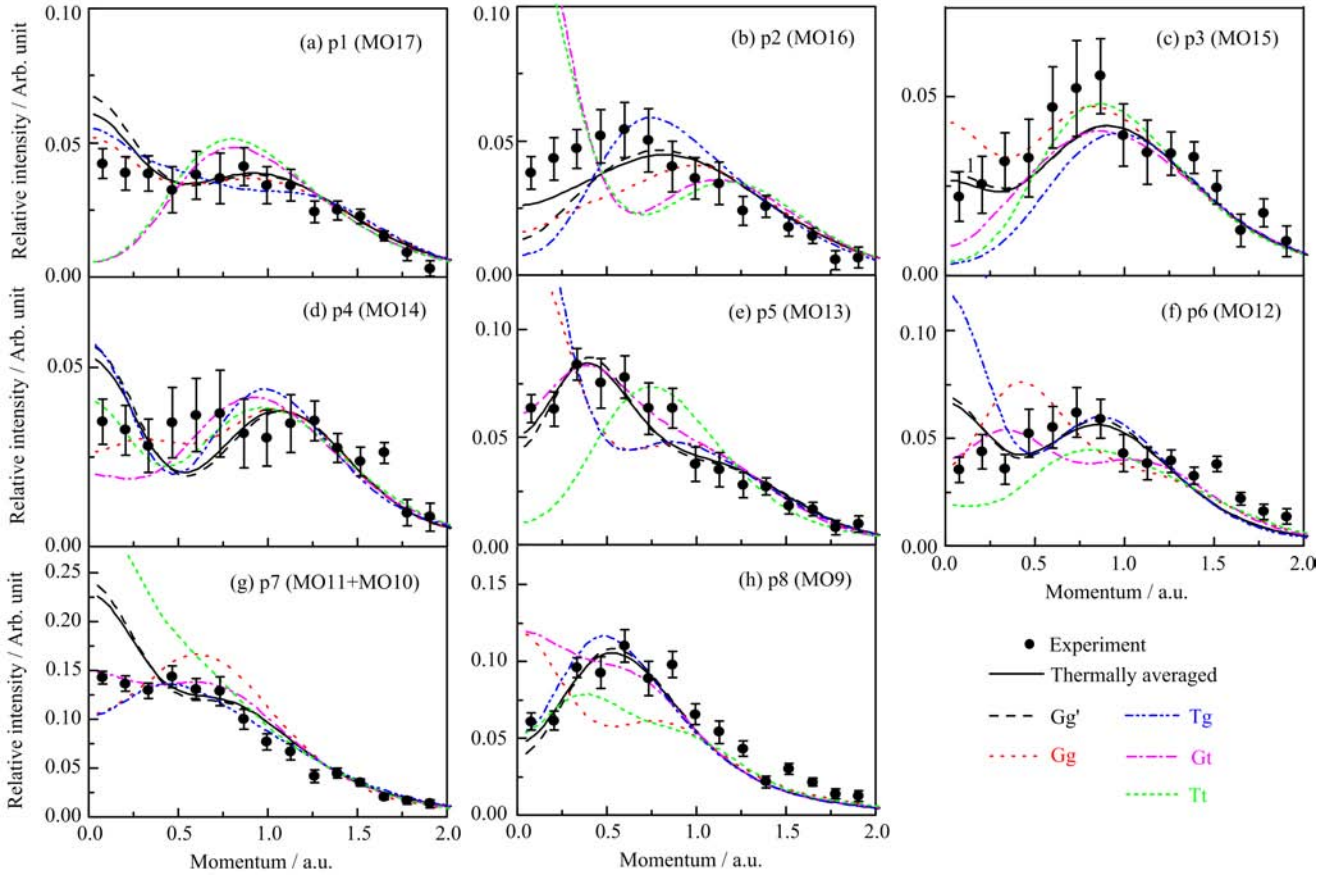

FIG. 3 Experimental momentum profiles (XMPs) and the corresponding thermally averaged theoretical momentum profiles (TMPs) for the outer valence MOs of 2-FE, along with the individual TMPs of each conformer for the corresponding MOs calculated by B3LYP/aug-cc-pVTZ.

actions between the oxygen lone pair and σ^*_{C-C} or σ^*_{C-H} bonds. Such interactions can induce a charge transfer from the oxygen to σ^*_{C-C} or σ^*_{C-H} bonds, and make the HOMOs of conformers having different components and orbital symmetries. As illustrated in Fig.4, the HOMO (*i.e.*, MO17) for *gauche* conformer Gg′, Gg, or Tg is composed of oxygen lone pair, σ_{C-C} and σ_{C-H} components. While for *trans* conformer Gt or Tt the HOMO is a pseudo-π orbital formed by oxygen lone pair and two reverse-phased σ_{C-H} components. Such differences of orbital components in position space become well-marked in momentum space, yielding two kinds of remarkably different TMPs, *i.e.*, 'p-type' profile and hybrid 'sp-type' profile, as shown in Fig.3(a).

The XMP for p2 and the TMPs for MO16 for various conformers are shown in Fig.3(b). It can be seen that the individual TMPs for *gauche* (Gg′, Gg and Tg) exhibits mainly 'p-type' characters while the TMPs for trans (Gt and Tt) are 'sp-type' profiles. The thermally averaged TMP shows a 'p-type' character, in line with the XMP for p2 in shape, but underestimates the experimental intensity in the low momentum region. Figure 3(c) compares the XMP for p3 with the TMPs for MO15. The individual TMPs of five conformers both display 'p-type' feature except for those of Gg′ and Gg appearing a 'turn up' intensity at p<0.25 a.u. In general, the thermally averaged TMP agreed well with the XMP for p3 in shape. As for the observed high intensity in Fig.3 (b) and (c), it may be contributed from distorted wave effects in view of the pseudo-π bond character of MO16 and MO15 illustrated in Fig.4. Such π-like MOs were often observed higher intensity than the PWIA calculations at low momentum region according to previous EMS studies [15, 47–49].

In Fig.3(d), we plot the XMP for p4 and the corresponding TMPs for MO14. This peak cannot be resolved and lies in the valley of two bands as shown in Fig.2(b). The large overlaps with p3 and p5 make the XMP data of p4 scattered. The thermally averaged TMP shows an 'sp-type' profile and could interpret the XMP qualitatively. For p5 and p6, as shown in Fig.3 (e) and (f), the thermally averaged TMPs of MO13 and MO12 can reproduce the XMPs well.

For p7 and p8, as we have mentioned above, according to the OVGF calculation, the peak p7 at 17.4 eV includes the cooperative contribution from MO11 and MO10, and the one (p8) at 18.3 eV is MO9. Therefore, we arrange the summed TMPs of MO11 and MO10 to

DOI:10.1063/1674-0068/28/cjcp1410175

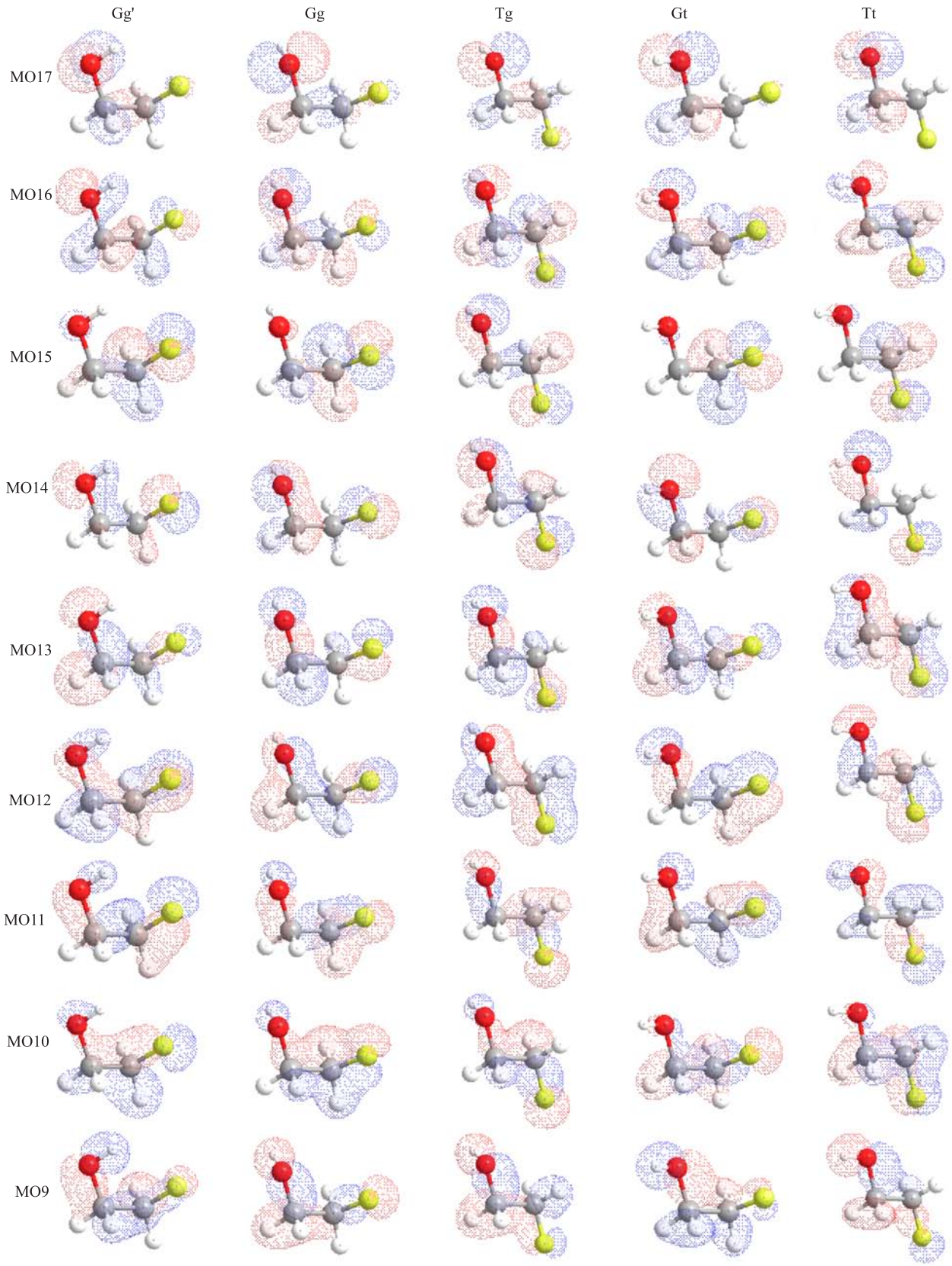

FIG. 4 The orbital maps in position space of nine outer valence MOs for the five conformers of 2-FE calculated by B3LYP/aug-cc-pVTZ.

DOI:10.1063/1674-0068/28/cjcp1410175

compare with the XMP of p7 in Fig.3(g), and the TMPs of MO9 to compare with the XMP of p8 in Fig.3(h). One can see that agreements between the TMPs and the XMPs have been achieved, which further confirm our assignments of the bands at 17.4 and 18.3 eV in the present BES and the previous PES. In addition, as shown in Fig.3(g), a noticeable difference between the XMP and the summed TMP remains at low momentum region (p<0.35 a.u.). One possible explanation is the change of molecular structures in the process of electron impact, such as isomerization or transition structures which departures from equilibrium conformers, leading to a noticeably populated change of conformers. The similar photo-isomerization induced by the C−H and O−H vibrational excitations has been reported [50]. If increasing the abundance of Gt conformer, in general, the agreement of XMPs and TMPs in Fig.3 can be improved in some extent.

IV. CONCLUSION

We report the first EMS measurement on outer valence-shell binding energy spectra and electron momentum profiles for gaseous 2-FE. The experiment results are interpreted on the basis of quantitative calculations of the ionization energies and of the related Kohn-Sham molecular orbitals at benchmark theoretical levels using OVGF and B3LYP methods. The experimental momentum profiles are generally consistent with the theoretical ones except in the lower momentum region. Furthermore, according to the EMS measurement combined with the theoretical calculations, the observed bands ionized from the outer valence orbitals of 2-FE have been assigned for the first time.

As for the discrepancy remained between experiment and theory, in practice, the interpretation of EMS experiments is subject to numerous complications such as the validity of PWIA in collision process [15, 47–49], the isomerization induced by the C-H and O−H vibrational excitations [50], the thermally induced nuclear dynamics involving all internal degrees of freedom in the electronic initial (neutral) ground state [20], and possibly ultra-fast nuclear dynamics in the final ionized state [11, 14], in the form of Jahn-Teller distortions [51], as well as possible bond breaking in the final ionized state [52]. This deserves to further explore in view of the aspects of complications both experimentally and theoretically, especially for structurally flexible molecules.

V. ACKNOWLEDGMENTS

This work was supported by the National Basic Research Program of China (No.2010CB923301) and the National Natural Science Foundation of China (No.11327404, No.20973160, No.10904136). The authors also gratefully acknowledge Professor C. E. Brion from the University of British Columbia (UBC) in Canada for giving us the HEMS programs.

[1] I. E. McCarthy and E. Weigold, Rep. Prog. Phys. **54**, 789 (1991).
[2] C. E. Brion, Int. J. Quant. Chem. **29**, 1397 (1986)
[3] M. A. Coplan, J. H. Moore, and J. P. Doering, Rev. Mod. Phys. **66**, 985 (1994).
[4] E. Weigold and I. E. Mac Carthy, *Electron Momentum Spectroscopy*, New York: Kluwer Academic/Plenum Publishers, (1999).
[5] Y. Zheng, J. J. Neville, and C. E. Brion, Science **270**, 786 (1995).
[6] J. J. Neville, Y. Zheng, and C. E. Brion, J. Am. Chem. Soc. **118**, 10533 (1996).
[7] W. N. Pang, J. F. Gao, C. J. Ruan, R. C. Shang, A. B. Trofimov, and M. S. Deleuze, J. Chem. Phys. **112**, 8043 (2000).
[8] M. S. Deleuze, W. N. Pang, A. Salam, and R. C. Shang, J. Am. Chem. Soc. **123**, 4049 (2001).
[9] X. J. Chen, F. Wu, X. Shan, and K. Z. Xu, J. Phys: Conf. Ser. **80**, 012003 (2007).
[10] F. Wu, X. J. Chen, X. Shan, S. X. Tian, Z. J. Li, and K. Z. Xu, J. Phys. Chem. A **112**, 4360 (2008).
[11] S. H. R. Shojaei, J. Vandenbussche, M. S. Deleuze, and P. Bultinck, J. Phys. Chem. A **117**, 8388 (2013).
[12] T. Yang, G. L. Su, C. G. Ning, J. K. Deng, F. Wang, S. F. Zhang, X. G. Ren, and Y. R. Huang, J. Phys. Chem. A **111**, 4927 (2007).
[13] C. G. Ning, Y. R. Huang, S. F. Zhang, J. K. Deng, K. Liu, Z. H. Luo, and F. Wang, J. Phys. Chem. A **112**, 11078 (2008).
[14] S. H. R. Shojaei, F. Morini, and M. S. Deleuze, J. Phys. Chem. A **117**, 1918 (2013).
[15] M. Yan, X. Shan, F. Wu, X. X. Xia, K. D. Wang, K. Z. Xu, and X. J. Chen, J. Phys. Chem. A **113**, 507 (2009).
[16] X. X. Xue, M. Yan, F. Wu, X. Shan, K. Z. Xu, and X. J. Chen, Chin. J. Chem. Phys. **21**, 515 (2008).
[17] X. J. Chen, F. Wu, M. Yan, H. B. Li, S. X. Tian, X. Shan, K. D. Wang, Z. J. Li, and K. Z. Xu, Chem. Phys. Lett. **472**, 19 (2009).
[18] C. G. Ning, Z. H. Luo, Y. R. Huang, B. Hajgat, F. Morini, K. Liu, S. F. Zhang, J. K. Deng, and M. Deleuze, J. Phys. B **41**, 175103 (2008).
[19] F. Morini, B. Hajgató, M. S. Deleuze, C. G. Ning, and J. K. Deng, J. Phys. Chem. A **112**, 9083 (2008).
[20] B. Hajgató, M. S. Deleuze, and F. Morini, J. Phys. Chem. A **113**, 7138 (2009).
[21] T. Scharge, C. Emmeluth, T. Häber, and M. A. Suhm, J. Mol. Struct. **786**, 86 (2006).
[22] F. R. Souza and M. P. Freitas, Comput. Theor. Chem. **964**, 155 (2011).
[23] J. M. Bakke, L. H. Bjerkeseth, T. E. Rønnow, and K. Steinsvoll, J. Mol. Struct. **321**, 205 (1994).
[24] J. Durig, P. Klaeboe, G. A. Guirgis, L. Wang, and J. Liu, Z. Phys. Chem. **191**, 23 (1995).
[25] K. Hagen and K. Hedberg, J. Am. Chem. Soc. **95**, 8263 (1973).
[26] J. Huang and K. Hedberg, J. Am. Chem. Soc. **111**, 6909 (1989).
[27] K. S. Buckton and R. G. Azrak, J. Chem. Phys. **52**, 5652 (1970).
[28] D. Davenport and M. Schwartz, J. Mol. Struct. **50**, 259 (1978).

DOI:10.1063/1674-0068/28/cjcp1410175

[29] M. Alaee and N. P. C. Westwood, J. Phys. Chem. **98**, 3818 (1994).
[30] X. J. Chen, L. X. Zhou, X. H. Zhang, X. F. Yin, C. K. Xu, X. Shan, Z. Wei, and K. Z. Xu, J. Chem. Phys. **120**, 7933 (2004).
[31] M. Takahashi, R. Ogino, and Y. Udagawa, Chem. Phys. Lett. **288**, 821 (1998).
[32] C. G. Ning, X. G. Ren, J. K. Deng, G. L. Su, S. F. Zhang, F. Huang, and G. Q. Li, Chin. Phys. **14**, 2467 (2005).
[33] X. Shan, X. J. Chen, L. X. Zhou, Z. J. Li, T. Liu, X. X. Xue, and K. Z. Xu, J. Chem. Phys. **125**, 154307 (2006).
[34] L. Cederbaum, J. Phys. B **8**, 290 (1975).
[35] W. Von Niessen, J. Schirmer, and L. Cederbaum, Comput. Phys. Rep. **1**, 57 (1984).
[36] V. Zakrzewski, J. Ortiz, J. A. Nichols, D. Heryadi, D. L. Yeager, and J. T. Golab, Int. J. Quantum. Chem. **60**, 29 (1996).
[37] C. Lee, W. Yang, and R. G. Parr, Phys. Rev. B **37**, 785 (1988).
[38] A. D. Becke, J. Chem. Phys. **98**, 5648 (1993).
[39] P. Duffy, D. P. Chong, M. E. Casida, and D. R. Salahub, Phys. Rev. A **50**, 4707 (1994).
[40] M. E. Casida, Phys. Rev. A **51**, 2005 (1995).
[41] X. J. Chen, X. Shan, and K. Z. Xu, *Nanoscale Interactions and Their Applications: Essays in Honour of Ian Mccarthy*, Kerala: Transworld Research Network, 37 (2007).
[42] C. Møller and M. S. Plesset, Phys. Rev. **46**, 0618 (1934).
[43] R. A. Kendall, T. H. Dunning, and R. J. Harrison, J. Chem. Phys. **96**, 6796 (1992).
[44] M. J. Frisch, G. W. Trucks, H. B. Schlegel, G. E. Scuseria, M. A. Robb, J. R. Cheeseman, J. A. Jr. Montgomery, T. Vreven, K. N. Kudin, J. C. Burant, J. M. Millam, S. S. Iyengar, J. Tomasi, V. Barone, B. Mennucci, M. Cossi, G. Scalmani, N. Rega, G. A. Petersson, H. Nakatsuji, M. Hada, M. Ehara, K. Toyota, R. Fukuda, J. Hasegawa, M. Ishida, T. Nakajima, Y. Honda, O. Kitao, H. Nakai, M. Klene, X. Li, J. E. Knox, H. P. Hratchian, J. B. Cross, C. Adamo, J. Jaramillo, R. Gomperts, R. E. Stratmann, O. Yazyev, A. J. Austin, R. Cammi, C. Pomelli, J. W. Ochterski, P. Y. Ayala, K. Morokuma, G. A. Voth, P. Salvador, J. J. Dannenberg, V. G. Zakrzewski, S. Dapprich, A. D. Daniels, M. C. Strain, Ö. Farkas, D. K. Malick, A. D. Rabuck, K. Raghavachari, J. B. Foresman, J. V. Ortiz, Q. Cui, A. G. Baboul, S. Clifford, J. Cioslowski, B. B. Stefanov, G. Liu, A. Liashenko, P. Piskorz, I. Komaromi, R. L. Martin, D. J. Fox, T. Keith, M. A. Al-Laham, C. Y. Peng, A. Nanayakkara, M. Challacombe, P. M. W. Gill, B. Johnson, W. Chen, M. W. Wong, C. Gonzalez, and J. A. Pople, *Gaussian 03, Revision B.04*, Pittsburgh PA: Gaussian Inc., (2003).
[45] P. Duffy, M. E. Cassida, C. E. Brion, and D. P. Chong, Chem. Phys. **159**, 347 (1992).
[46] X. J. Wu, *Ph. D. Dissertation*, Hefei: University of Science and Technology of China, (2005).
[47] C. E. Brion, Y. Zheng, J. Rolke, J. J. Neville, I. E. McCarthy, and J. J. Wang, J. Phys. B **31**, L223 (1998).
[48] I. V. Litvinyuk, Y. Zheng, and C. E. Brion, Chem. Phys. **253**, 41 (2000).
[49] X. G. Ren, C. G. Ning, J. K. Deng, S. F. Zhang, G. L. Su, F. Huang, and G. Q. Li, Phys. Rev. Lett. **94**, 163201 (2005).
[50] C. L. Brummel, S. W. Mork, and L. A. Philips, J. Chem. Phys. **95**, 7041 (1991), and references therein.
[51] Z. J. Li, X. J. Chen, X. Shan, T. Liu, and K. Z. Xu, J. Chem. Phys. **130**, 054302 (2009).
[52] Y. F. Shi, X. Shan, E. L. Wang, H. J. Yang, W. Zhang, and X. J. Chen, J. Phys. Chem. A **118**, 4484 (2014).

DOI:10.1063/1674-0068/28/cjcp1410175